

N91-11687

p74

A PROPOSED DEFINITION FOR A PITCH ATTITUDE TARGET FOR THE MICROBURST ESCAPE MANEUVER

Richard S Bray
NASA Ames Research Center
Moffett Field, California

SUMMARY

The Windshear Training Aid promulgated by the FAA defines the practical recovery maneuver following a microburst encounter as application of maximum thrust accompanied by rotation to an aircraft-specific target pitch attitude. In search of a simple method of determining this target, appropriate to a variety of aircraft types, a computer simulation was used to explore the suitability of a pitch target equal in numerical value to that of the angle of attack associated with stall warning. For the configurations and critical microburst shears simulated, this pitch target was demonstrated to be close to optimum.

BACKGROUND

In January, 1987, the FAA released the Windshear Training Aid (reference 1), a package of documentation and visual materials defining procedures and contents of a recommended training course for pilots on the subject of microburst wind shear. The primary target of this effort was the civil air-transport community, and the material was derived and presented in the context of the operation of large jet transport aircraft. While most of the extensive educational material contained in the documents was not aircraft-specific in nature, those sections dealing with escape from microburst encounters, and especially the simulator training programs, specifically considered the B-727 aircraft.

It is recommended in Reference 1 that, upon recognition of encounter with a severe wind shear, the pilot should command full thrust and rotate the aircraft to a specified target pitch attitude. In the supporting documentation, the procedure used in defining this pitch target for the B-727 is described. The process consisted of determining the attitude that resulted in survival in the strongest shear, with a minimum exposure to a stall-warning angle-of-attack condition. This was accomplished with the use of a mathematical model of the aircraft in computations of trajectories resulting from various pitch attitudes. The selected value, 15 degrees, was not described as related to any other aircraft-specific measure. More recently, Lockheed, using a similar approach, developed the recommendation that a pitch target of 17 degrees be used in the case of the L1011 aircraft. The documents imply that this same procedure be used for developing escape procedures for each aircraft type and model. The following paragraphs propose and discuss examination of a simpler pitch target definition that might be applied to any aircraft configuration.

THE PREMISE

It is noted that the pitch targets chosen for the B-727 and the L1011 crudely approximate the numerical values of the angles-of-attack associated with the activation of their stick-shaker stall warning systems. It is also noted that if it can be assumed that extended areas of strong downdraft cannot exist near the ground, even in a microburst, an aircraft cannot descend rapidly into the ground before experiencing stall warning if its pitch attitude is at or above the numerical value of stall-warning angle of attack. (Flight path angle = pitch angle minus angle

of attack). This paper reports an examination of the premise that a pitch target, effective for a range of aircraft characteristics, is represented by the numerical value of the stall-warning angle of attack.

PROCEDURE

The dynamic performance characteristics of three generic aircraft were defined for take-off and approach configurations in terms of wing loading, W/S, thrust-to-mass, T/m, and lift and drag. After establishing initial conditions, and defining pitch attitude and thrust for the recovery maneuver, the models were "flown" through a modelled microburst wind field using various pitch attitude targets in a procedure similar to that used in support of the Windshear Training Aid. When stall-warning angle of attack was encountered, pitch was reduced to avoid significant increase of angle of attack beyond that value. Details of the method of trajectory computation are included in Reference 2.

For each configuration, a microburst intensity was chosen that resulted in a marginal recovery using the "stall-warning angle of attack" pitch target. In the same microburst, trajectories were computed for lesser and greater recovery pitch attitudes, and the relative success, in terms of ground clearance and time near stall, were noted.

AIRCRAFT CONFIGURATIONS

Chosen for study were generic configurations representative of three categories of aircraft; a large, high-wing-loading jet transport incorporating high-lift leading edge slats; a jet-powered configuration of lower wing loading without leading-edge devices, and a turboprop-powered configuration, also without leading-edge devices. These latter two might be considered representative of some business jets and turboprop commuter aircraft respectively. The three aircraft were assumed to be twin-engined configurations, and they were not considered to be operating at full maximum gross weight; thus, they possessed large performance margins to help them recover from shear encounters. No special effort was made to exactly match the performance margins of these models because (1) they represented categories of aircraft that experience quite different operational situations, and (2) it was not the primary intent of this work to study their relative performance in wind shear. The three aircraft will be referred to as heavy jet (HJ), light jet (LJ), and turboprop (TP). The aircraft are described in Table 1, and the maximum thrust characteristics, which vary with speed, are defined in Figure 1.

MICROBURST MODEL

The wind fields were defined by the computational microburst model described in Reference 2. The model describes an axially symmetric downdraft column that is converted to a radially divergent outflow near the ground plane. Below a specified altitude at which divergence begins, vertical velocity reduces exponentially to zero at ground level. Considering volumetric continuity, the resultant peak horizontal divergence velocities (near the circumference of the downdraft column) increase linearly with altitude increment below the specified altitude; thus, the maximum divergence of the winds, and the maximum shear gradient, occurs near the ground. No specific vortex flow is defined, and no smaller scale turbulence is included. The amplitude of the divergence can be increased by either increasing the diameter of the microburst (holding gradient constant), or increasing the downdraft velocity (increasing gradient). For this work, the aircraft experiences winds as if it had flown directly through the center of the microburst. Basic characteristics of the microburst winds encountered by the models in this exercise are listed in Table 2.

INITIAL CONDITIONS

The initial conditions for the start of the trajectory computations were somewhat arbitrarily chosen, as was the relative position of the modelled microburst. For take-off, the aircraft was assumed to be at 50 feet established in normal climb at a speed of V_2+10 knots and just entering the headwind to tailwind shear. On approach, the aircraft was in a normal descent at 400 feet, about 10% above normal reference speed, and at reduced power, as if the aircraft had been experiencing an increasing head wind. The shear was encountered within the first two seconds. In all cases, the timing of the initiation of the recovery maneuver reflected an assumed delay in recognition of the shear, and in most cases 10 to 15 knots had been lost before action was initiated. In the approach cases, the rate of increase of thrust from its initial value to full thrust was intended to be representative of the powerplant type.

RESULTS AND DISCUSSION

The results of a typical trajectory computations are shown for a take-off shear encounter with the HJ model in Figure 2, and for a discontinued approach with the same model in Figure 3, in which the important variables are plotted versus horizontal distance. Note that the data points represent one-second intervals.

At the initiation of the take-off calculations (Figure 2), the aircraft is assumed to be entering the microburst shear at its trimmed climb attitude of 22 degrees. After a four-second delay, in which a loss of 15 knots of airspeed occurs, pitch attitude is reduced to the pitch target of 18 degrees. In the large shear gradient, speed continues to decay, and climb rate reduces to zero at an altitude of 335 ft. At this point, the aircraft is flying in a downdraft of 23 ft/sec. With continuing reduction in airspeed, angle of attack increases until stall warning is indicated at a value of 18 degrees. In response, pitch attitude is reduced to prevent angle of attack from increasing. After 4 seconds, the shear and downdraft end, and a rapid increase in airspeed begins. Over the next 6 seconds, recovery is made at a very low altitude at high angle of attack. As indicated earlier, the microburst severity was chosen to produce a marginal recovery with this pitch attitude target.

Similar events are seen in the approach case illustrated in Figure 3. The recognition delay, together with delay in thrust response, result in only a temporary delay in further descent, and recovery again occurs as the shear ends after the aircraft has suffered a period of about six seconds at stall-warning angle of attack.

Take-off trajectories:

The take-off trajectories for the three configurations, at various pitch attitudes, are shown in figures 4 through 6. The behavior of the HJ configuration is shown in figure 4. For this case, the breadth of the microburst shear was set at 4200 feet, and the higher altitude downdraft velocity was set at 60 feet/second. As was seen in Figure 2, for the pitch target of 18 degrees, the total horizontal shear experienced was 145 ft/sec (86 knots), and the maximum downdraft encountered was 23 ft/sec. The other trajectories reflect the effects of the same microburst model configuration. It is seen that as the pitch target is increased to 21 degrees, nearly the same recovery altitude results. A slightly higher peak altitude is reached, but the time at limit angle of attack, the pitch down and peak descent rate are greater. Data not included in the figure indicate that further increases in pitch target produce even less favorable results. As illustrated in the figure, reducing the pitch target to 15 degrees

produces the favorable effects of lower airspeed loss and less time at limit angle of attack, but the recovery altitude is lower. Further reduction of target attitude results in ground contact.

The results for the LJ configuration are shown in figure 5. In this case, stall-warning occurs at 12 degrees, and the operational pitch attitudes are generally lower than in the previous model. Increasing the pitch target to 15 degrees results in an increase of 15 ft in recovery altitude, but at the expense of a considerably greater time at limit angle of attack, and a larger pitch-down to avoid stall. A pitch target of 9 degrees results in a recovery very close to the ground.

The performances of the TP configuration are shown in figure 6. The stall warning is assumed to occur at 11 degrees. The microburst intensity is approximately the same as for the previous configurations. Speeds and peak altitudes reflect the lower operational speed of this lighter wing-loading aircraft. Again, varying the pitch target above or below 11 degrees does not result in a net improvement in recovery performance.

Discontinued approach trajectories:

The discontinued approach trajectories for the three configurations, at various pitch attitudes, are shown in figures 7 through 9. The behavior of the HJ configuration is shown in figure 7. For this case, the breadth of the microburst shear was set at 4400 feet, and the higher altitude downdraft velocity was again set at 60 ft/sec. As was seen in Figure 3, for the pitch target of 18 degrees, the total horizontal shear experienced was 135 ft/sec (80 knots), and the maximum downdraft encountered was 22 ft/sec. The other trajectories reflect the effects of the same microburst model configuration. An increase of the pitch target from 18 to 22 degrees resulted in a failure to recover, while a decrease to 14 degrees produced a recovery altitude only slightly lower than that seen at 18 degrees while only approaching limit angle of attack.

The performances of the LJ configuration, in the same winds, are shown in Figure 8. The effects of varying target pitch attitude are seen to be very much as those seen with the previous configuration.

Performances for the TP configuration are shown in Figure 9. In this case, the stall-warning angle of attack is assumed to be 10 degrees. It is seen that reducing the pitch target to 8 degrees results in about the same recovery altitude as produced by an attitude of 10 degrees, and again with slightly more favorable angle of attack and speed histories. On the other hand, increasing the attitude target to 13 degrees results in more adverse performance in all respects.

The less adverse sensitivity to reduced pitch attitudes in the approach case is a result of the opportunity for the aircraft to exchange altitude for airspeed. It apparently does this more efficiently at slightly reduced attitudes. As the encounter altitude is lowered, it is expected that the results would more resemble those of the take-off case, which exhibited reduced adverse sensitivity to increased pitch attitudes.

CONCLUDING REMARKS

In search of a simple method of determining a wind-shear recovery pitch-attitude target, appropriate to a variety of aircraft types, a computer simulation was used to explore the suitability of a pitch target equal in numerical value to that of the angle of attack associated

with stall warning. In the case of encounter shortly after lift-off, recovery success was not adversely sensitive to small increases in target attitude above that proposed, but reductions in pitch target produced less than successful results. In the approach encounters, it was seen that the reverse trend prevailed. For the three aircraft configurations and the critical microburst shears simulated, the proposed pitch target was demonstrated to be close to optimum for both take-off and low-approach encounters.

REFERENCES

1. Windshear Training Aid, Federal Aviation Administration, Washington, D. C., 1987
2. Bray, Richard S.: Aircraft Performance and Control in Downburst Wind Shear, Paper No. 861698, SAE Aerospace Technology Conference, Long Beach, California, 1986.

Table 1: Aircraft characteristics

Definitions:

A	Angle-of-attack, deg
CL	Lift coefficient
CD	Drag coefficient
L/D	Lift/drag ratio
VREF	1.3*stall speed, knots
V2	Minimum speed, second-segment climb, knots
W/S	Wing loading, lb/ft ²

Characteristics:

HJ:	$CL = CL_0 + 0.095*A - 0.000025*A^3$
	$CD = CL/L/D$
	$L/D = L/D_0 + 0.9*A - 0.055*A^2 + 0.0007*A^3$
LJ:	$L/D = L/D_0 + 0.9*A - 0.07*A^2 + 0.0005*A^3P$
TP:	$CL = CL_0 + 0.10*A - 0.000025*A^3$
	$CD = CD_0 + 0.054*(CL - DELCL)^2 + FCLT*(T/m)$

		<u>Take-off</u>	<u>Approach</u>
HJ:	CL ₀	0.25	0.50
	L/D ₀	6.0	3.0
	W/S	110	90
	V2	152	
	VREF		136
	Stall warning A = 18 deg		
LJ:	CL ₀	0.25	0.50
	L/D ₀	6.0	3.0
	W/S	79	65
	V2	152	
	VREF		136
	Stall warning A = 12 deg		
TP:	CL ₀	0.3	0.7
	CD ₀	0.05	0.14
	W/S	40	40
	V2	110	
	VREF		110
	Stall warning A	11	10
	DELCL	0.3	0.5
FCLT	0.02	0.03	

Table 2: Microburst characteristics (based on model of reference 2)

	Diameter, ft	Downdraft, ft/sec (above 1500')	Max. divergence, knots
HJ and LJ:			
Take-off	4200	60	86
Approach	4400	60	80
TP:			
Take-off	4000	62.5	87
Approach	4000	60	74

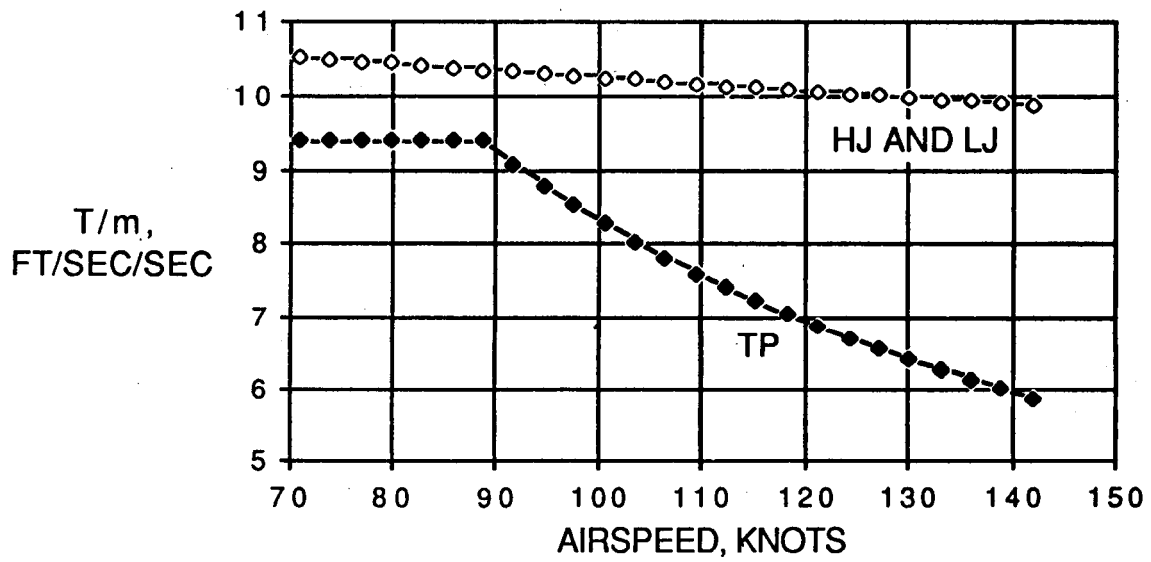
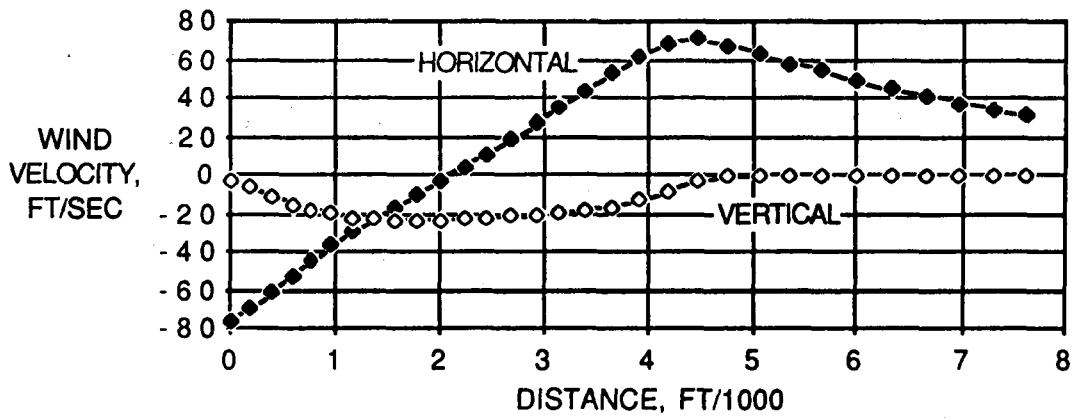
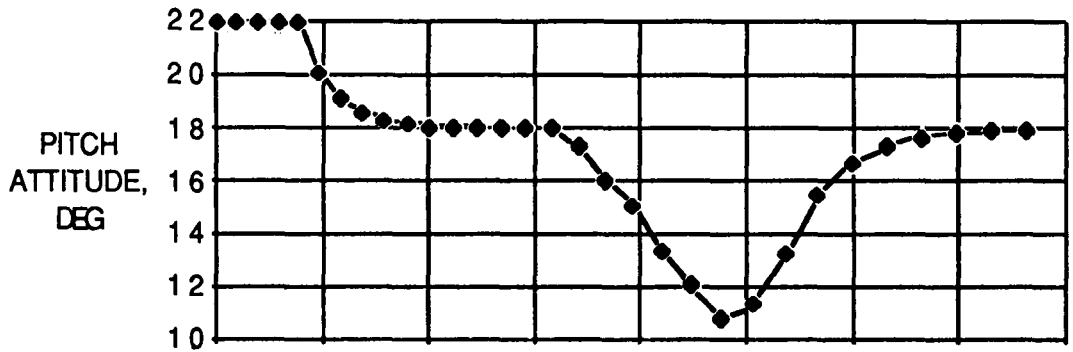
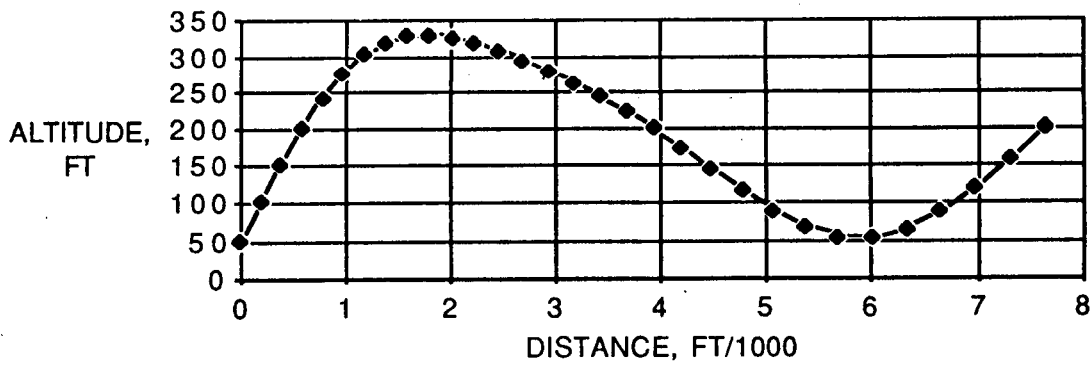
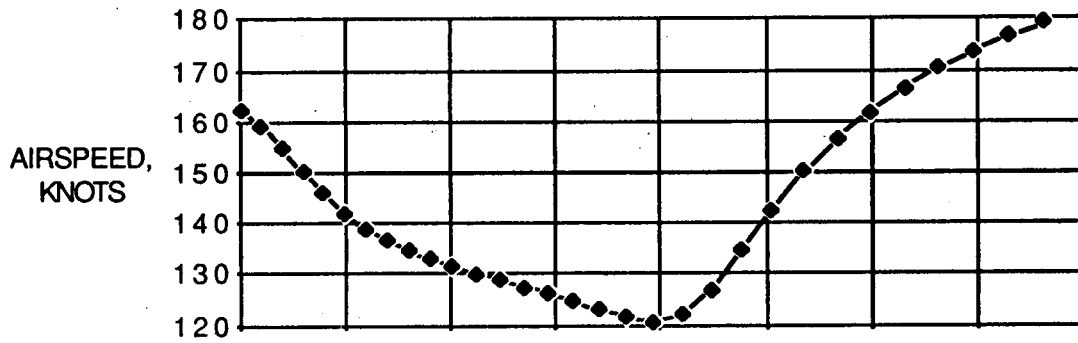
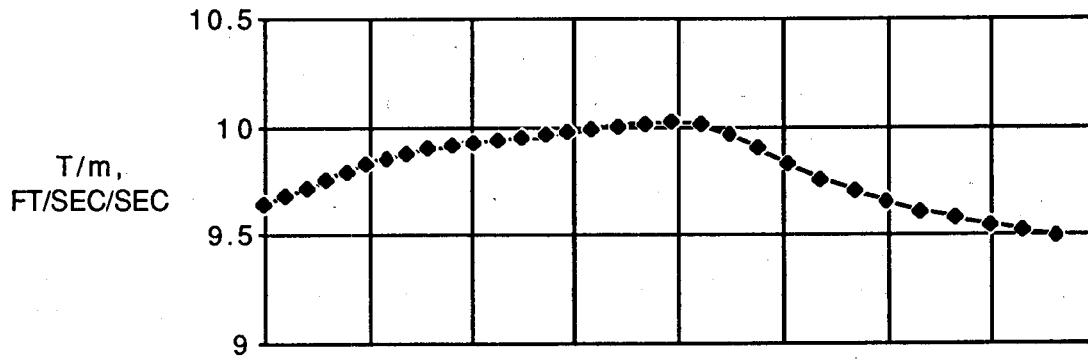


Figure 1. Variation with airspeed of acceleration due to thrust.



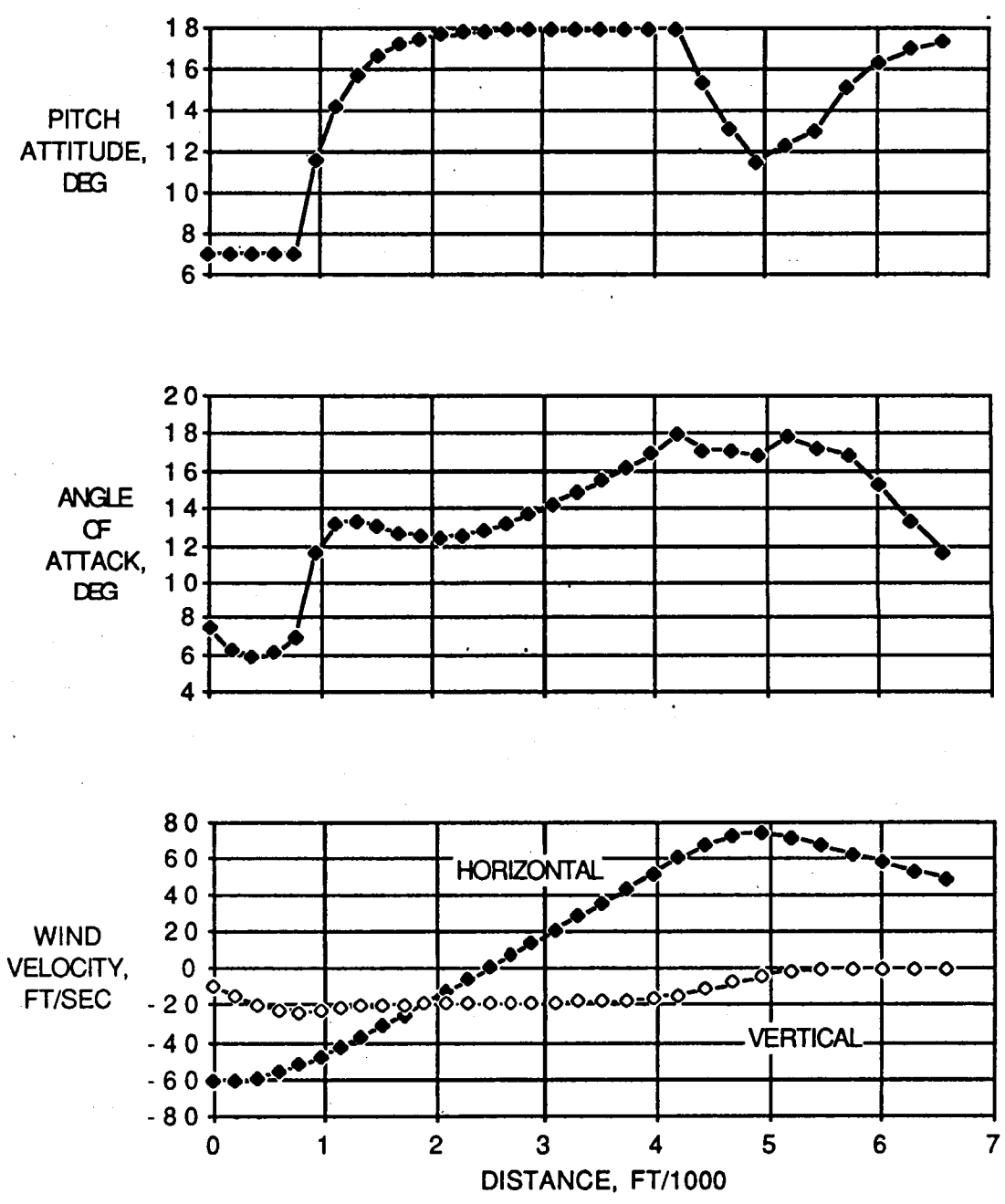
(a)

Figure 2. Performance of the HJ configuration in a take-off microburst encounter using a pitch target of 18 degrees.



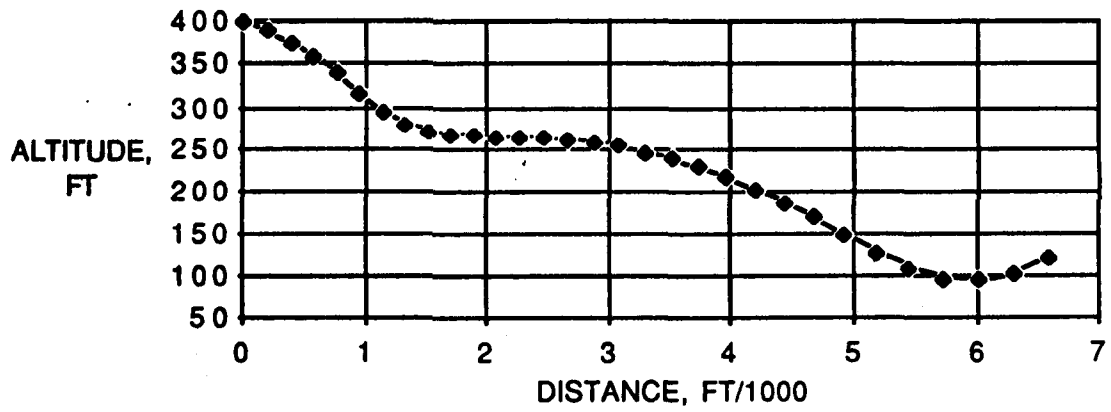
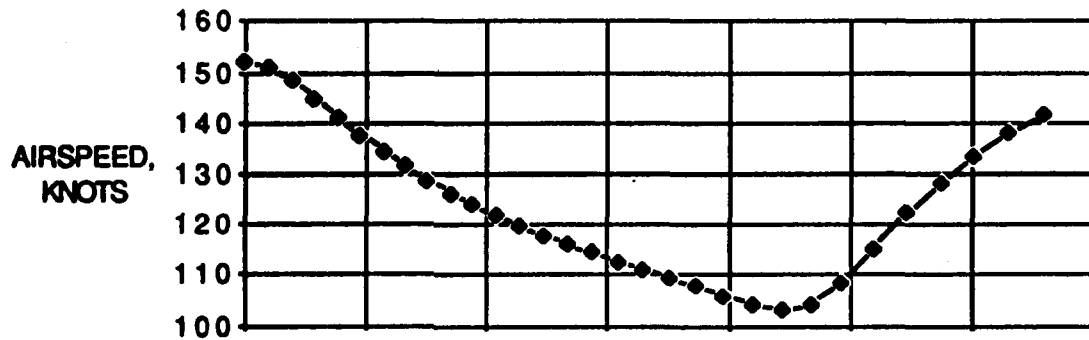
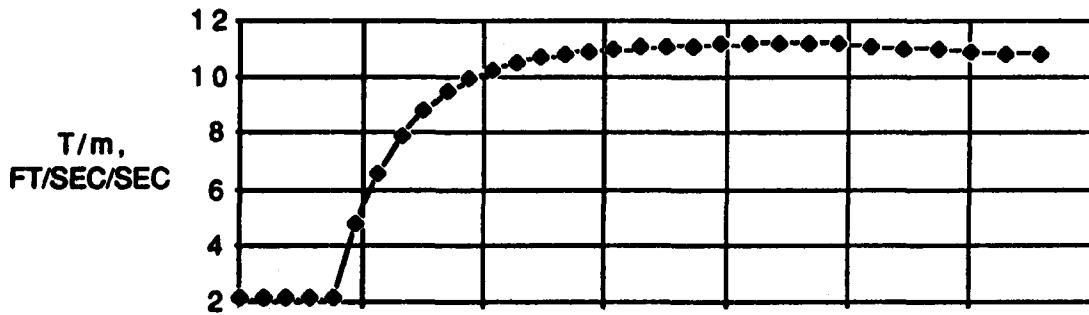
(b)

Figure 2. -continued.



(a)

Figure 3. Performance of the HJ configuration in a landing approach microburst encounter using a pitch attitude target of 18 degrees.



(b)

Figure 3. -continued.

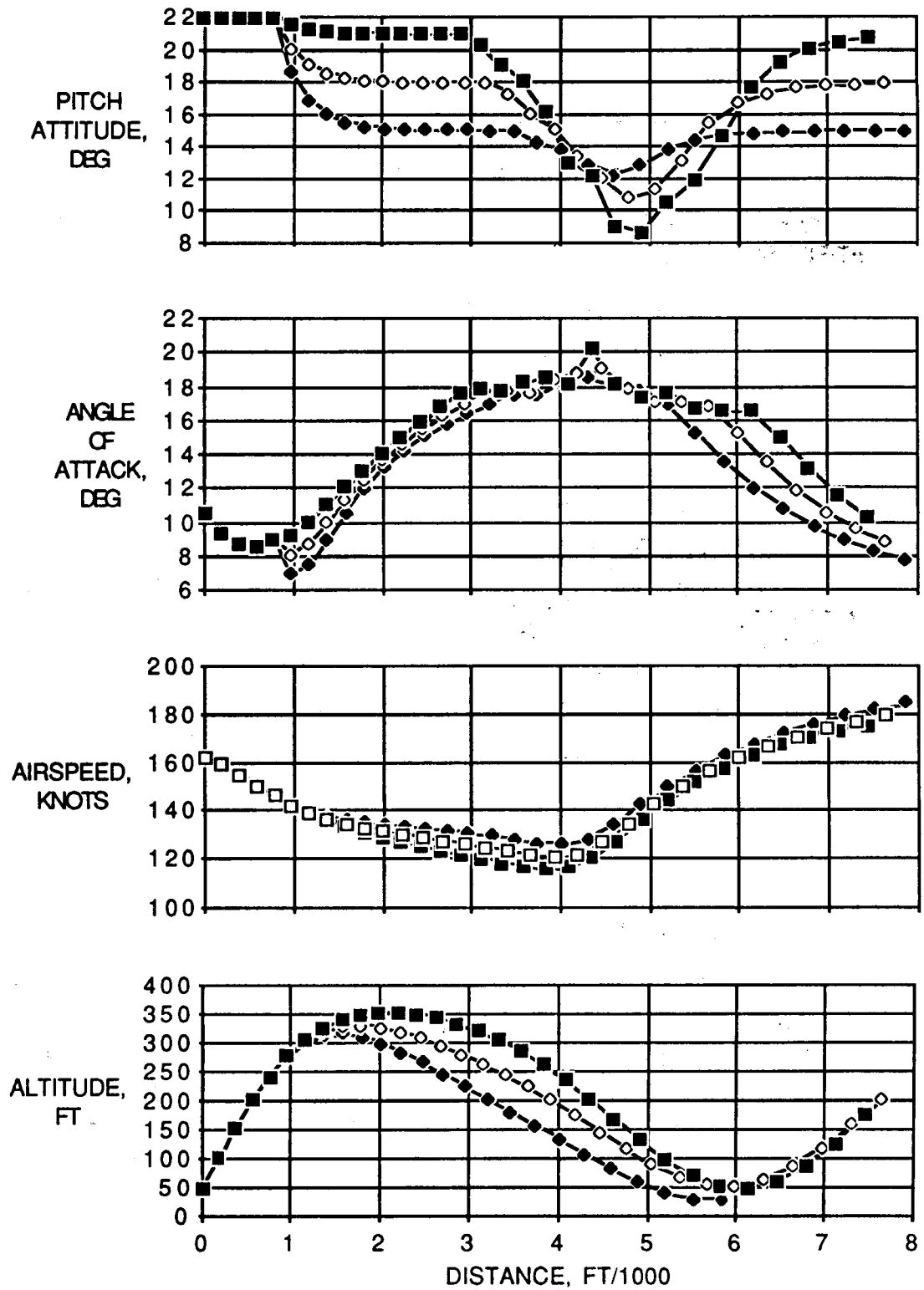


Figure 4. Performance of the HJ configuration in take-off microburst encounters.

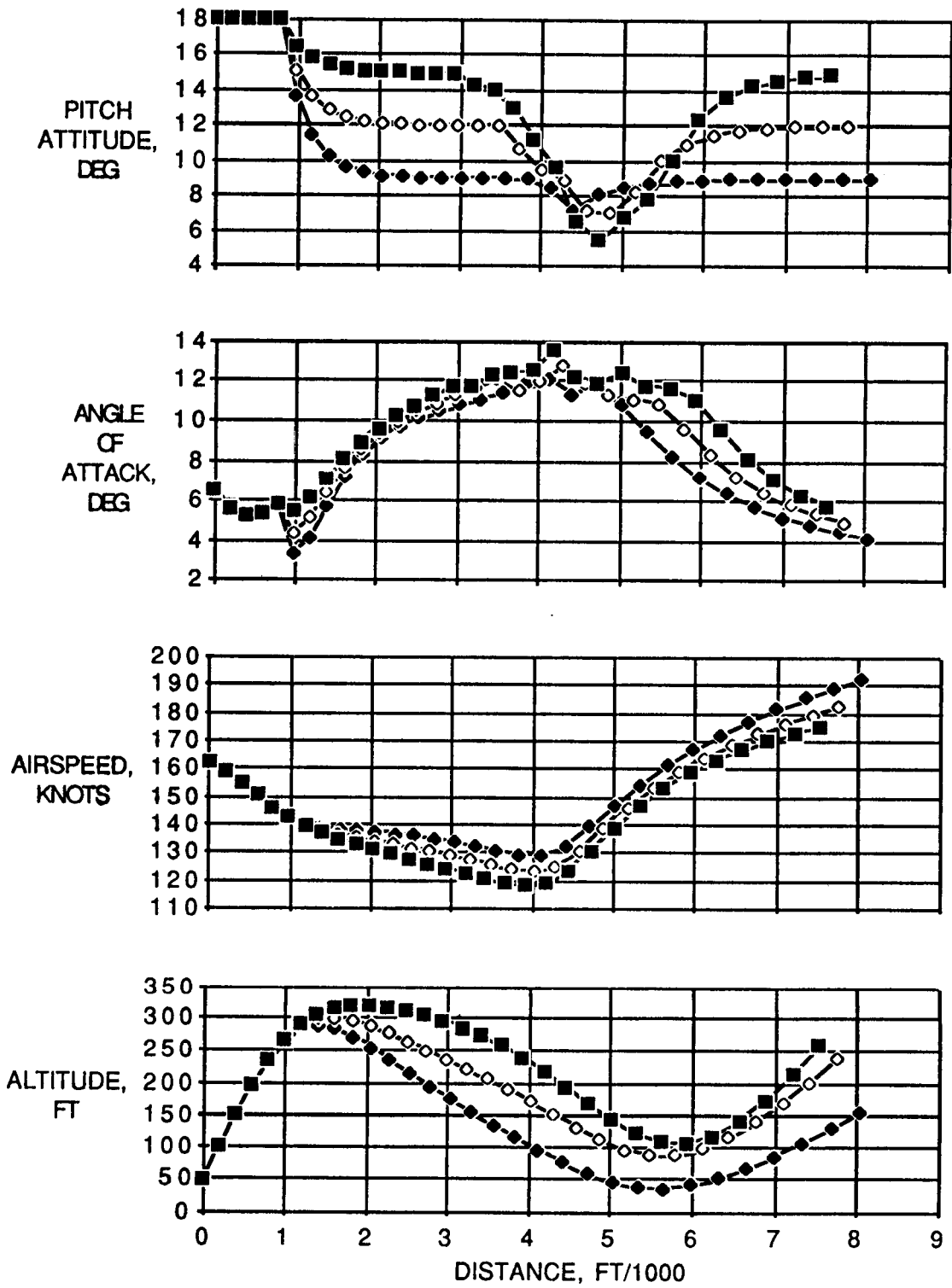


Figure 5. Performance of the LJ configuration in take-off microburst encounters.

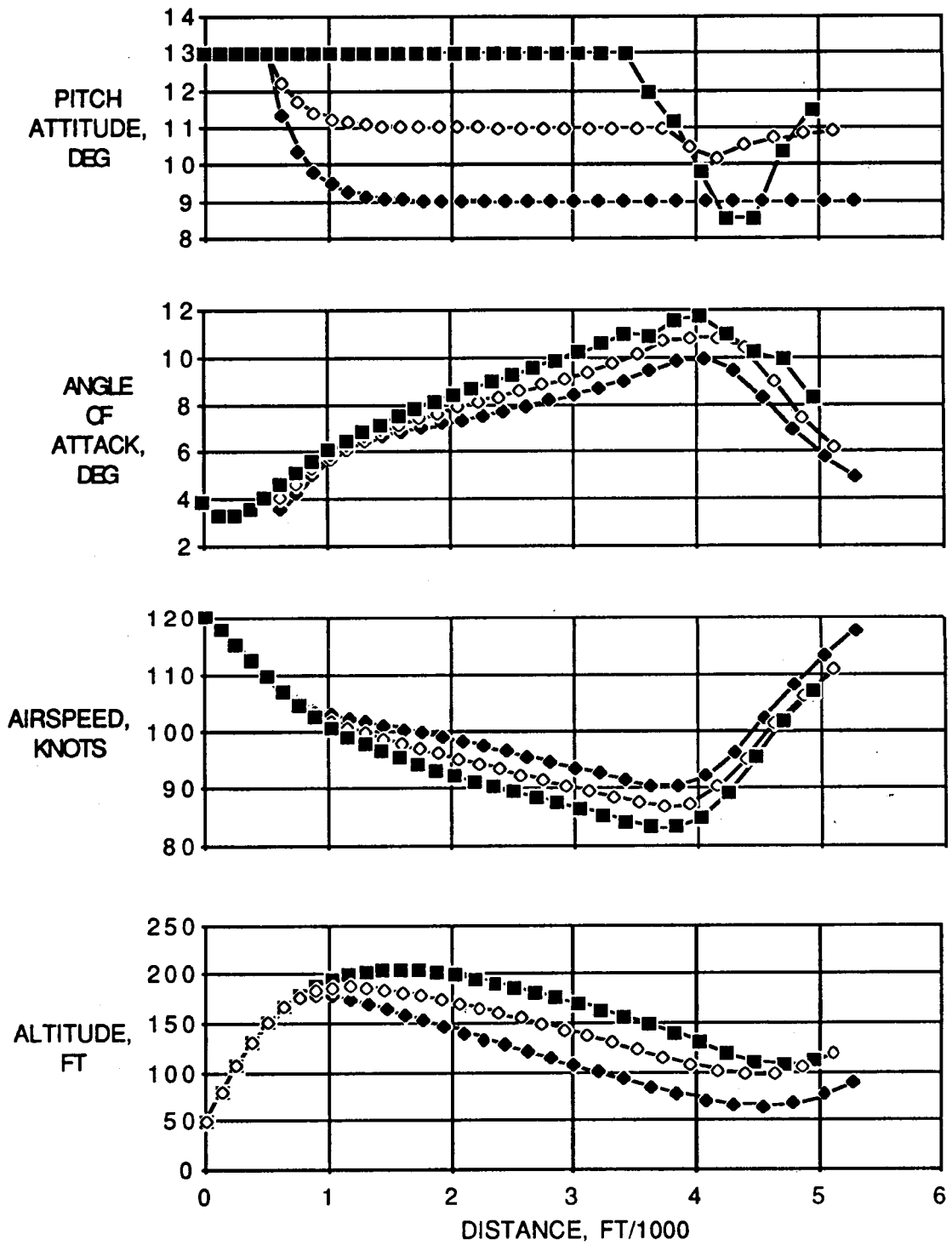


Figure 6. Performance of the TP configuration in take-off microburst encounters.

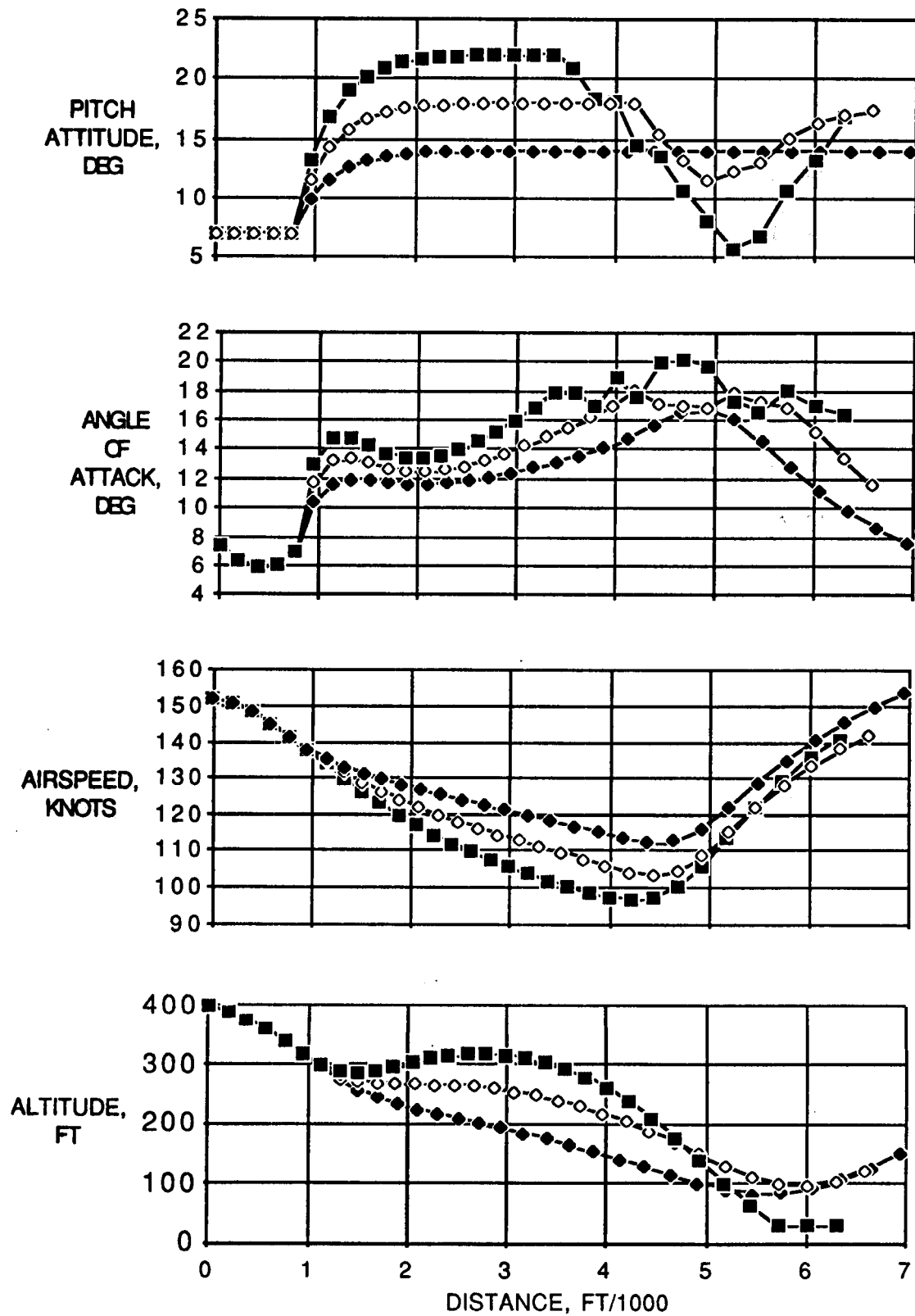


Figure 7. Performance of the HJ configuration in landing approach microburst encounters.

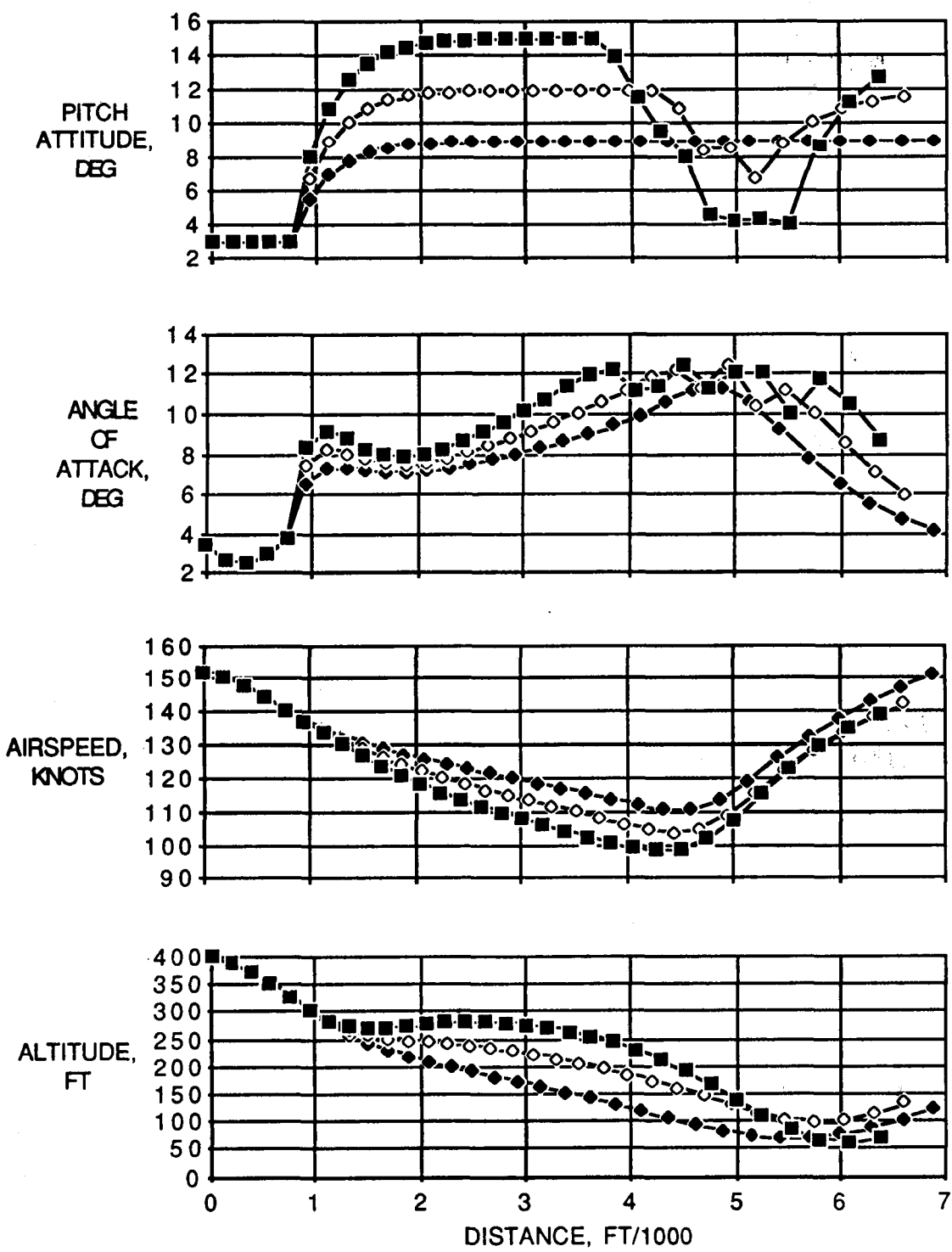


Figure 8. Performance of the LJ configuration in landing approach microburst encounters.

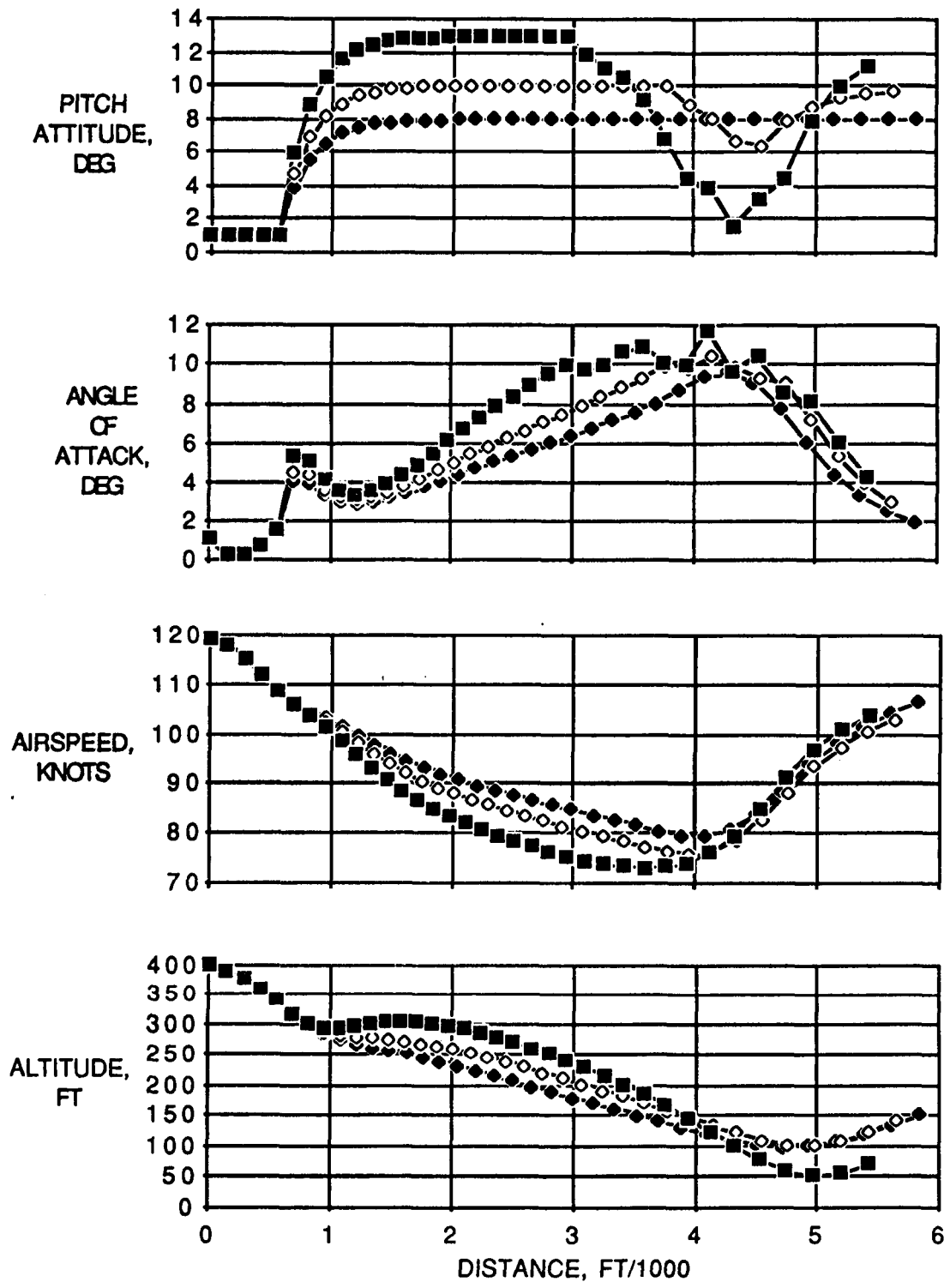


Figure 9 Performance of the TP configuration in landing approach microburst encounters.